Available online at www.elixirpublishers.com (Elixir International Journal)

Vibrational Spectroscopy

Elixir Vib. Spec. 84 (2015) 33511-33522

ISSN: 2229-712X

Ab Initio and Charge Density Analysis of Au and S Substituted Diclopentyl-Cyclohexane Molecular Nanowire

A. David Stephen[1], P.V. Nidhin[1] and P. Gnanamozhi[2]

[1]Department of Physics, Sri Shakthi Institute of Engineering and Technology, Coimbatore, India.

[2]Department of Physics, Nehru Memorial College, Tiruchirappalli, India.

ARTICLE INFO

Article history:

Received: 19 May 2015;

Received in revised form:

19 June 2015;

Accepted: 30 June 2015;

Keywords

Nanowire,
DFT-LANL2DZ,
Bond Topological Study,
MO Analysis,
Electrostaic Potential,
I-V Characteistics.

ABSTRACT

The Ab-initio and charge density analysis of Au and thiol substituted Dicyclopentyl-Cyclohexan (DCC) molecular nanowire, was carried out using high level Density Functional Theory (DFT) with the help of LANL2DZ basis set coupled with the Bader's theory of atoms in molecules . All the studies were carried out in the presence of an applied electric field which is gradually increasing from 0.05–0.26VÅ^{-1}. The effect of the applied electric field on the geometrical and the topological analysis of the molecular wire is thoroughly made and studies were made to charcterise the bonds, especially the terminal bonds, which shows ionic nature. The variation in the dipole moment as a consequence of the polarization caused by the applied EF is thoroughly studied. HOMO-LUMO analysis was carried out to determine the way the molecule interacts with other species which may initiates the conductivity. The I–V characteristics of the molecule have been studied for various applied fields for finding the conducting nature of the molecule-electrode-molecule system. The molecular electrostatic potential surface was plotted over the geometry of the molecule to elucidate the reactivity of the molecule.

Introduction

The designing of nanowires and conducting nanomaterials were found to be advanced theoretical studies of the present age, for which the adequate and important input were derived from the theoretical and experimental investigations in the corresponding field [1]. The role of nanowires in nanodevices was more significant, so that the designing of such conducting structures also find its importance. The electrical conductivity of such molecules mainly depends on their molecular structure, and its charge density distribution [2]. It was stated that the coupling of certain elements may vary the conducting properties of such molecules drastically. The coupling effect of donor and acceptor termini of DCC (Diclopentyl-cyclohexane) make the molecule to exhibits a wire like characteristics [3]. The coupling effect can be made, as noted before, by the attachments of electrodes over the molecule (electrode-molecule-electrode system) [4]. The delocalisation of electrons were made the molecules better conductor [5,6]. The energy gap between the highest occupied molecular orbital (HOMO) and the lowest unoccupied molecular orbital (LUMO) shows the behaviour of conducting nano wire. But the complete understanding of the charge transport mechanism in the coupling junctions through experimental aspects is really a challenging problem because of many uncontrollable experimental parameters.

In that cases the theoretical quantum chemical calculations have found to the better solutions. In the present study, the charge density and mainly the electrical characteristics of Au and S substituted DCC molecule. Figure 1 have been analyzed in the presence of a gradually increasing electrical field (EF) on the basis of theoretical charge density analysis and also quantum chemical calculations coupled with AIM theory [7]. The conductivity of the molecules at various applied field is also analysed using the I-V characteristics curve.

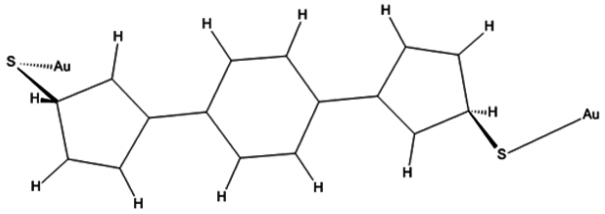

Figure 1. Au and S substituted Dicyclopentyl-Cyclohexane molecule

Computational details

The optimization of Au and thiol substituted DCC molecule was done for the gradually increasing applied field of five biasing steps 0.05, 0.10, 0.18, 0.21, 0.26 VÅ^{-1} by Density Functional Theory (DFT) method using Gaussian03 program package [8]. The whole DFT calculations were carried out by the application of Becke's three parameters exchange function and Lee, Yang and Parr gradient-corrected correlation function (B3LYP hybrid function) along with LANL2DZ (Los Alamos National Laboratory of Double Zeta) basis set, which gives the detailed effect of heavy metal atoms in a molecule [9]. All the geometry optimizations were carried out via Berny algorithm in redundant internal coordinates with the threshold convergence for maximum force, root mean square (RMS) force, maximum displacement and root mean square (RMS) displacement are 0.00045, 0.0003, 0.001 and 0.0012 au respectively.

The electron density $\rho_{bcp}(r)$, Laplacian of electron density $\nabla^2\rho_{bcp}(r)$, bond ellipticity ε and the eigenvalues λ_i were calculated for various applied field using EXT94b routine incorporated to the AIMPAC software [10]. The Laplacian of charge density and the deformation density maps were plotted using DENPROP and wfn2plots program packages. The

Tele: +919952273932
E-mail addresses: davidstephen_dav@yahoo.co.in

HOMO-LUMO and Electrostatic potential (ESP) maps were plotted using GVIEW [8]. The GaussSum program has been used to determine the density of states (DOS) at various levels of applied Electric fields [11].

Results and discussion

Structural aspects

The current study deals with the effect of EF over the topological nature of the electrode-molecule-electrode system. Figure 2 shows the complete optimized geometry of DCC molecular wire for the zero and applied, gradually increasing electric filed. This molecule under consideration has one central aromatic ring and the Au atoms are attached at the ends of the molecule through thiol atoms which makes a electrode-molecule-electrode system. The coupling effect in the metal junctions can be due to the good link of thiol atom with the molecule and Au. It has been noted that the effect of an external electric field may alter the geometrical as well as the eletron transport nature of the molecules [12]. Thus the present study reveals the gradual variations in topological and geometrical nature of the molecule with the effect of applied field ranging from 0 to 0.26 VÅ^{-1}.

On observing the three ring structures (cyclopentane and cyclohexane) under applied field and zero field effects, the C−C bond distances in the molecule varies from 1.360 to 1.514, the maximum observed variation is 0.008 Å. As the field increases the connector bond C−C distances is decreased from 1.475 to 1.469. The zero field distances of S−C bonds are ~1.930 Å; as the field increases, these distances are decreased with maximum variation of 0.0045. In the left−end (L), the distance decreased from 1.925 to 1.923 Å, while in the right−end (R), the distance decreases from 1.935 to 1.933 Å; the variation in the both R−end and L−end are found to be equal, which is ~ 0.02Å. The zero and the applied field distances of Au−S bonds are found unequal. As the field increases, the R−end Au−S bond distance increases from 2.931 to 2.405 Å; notably, there is no variation in L−end for all the applied fields. And, for the maximum applied field (0.26 VÅ^{-1}), the distance at L− and R−ends are 2.427 and 2.386 Å respectively. This large difference is attributed to the applied field lengthening the Au−S bond through by shrinking the S−C bond distance in the wire Table 1. However, the zero field (1.101 Å) and higher field (~1.085 Å) C−H bond lengths, remains same with the increase of field. Table 1 shows the complete bond length values of Au and S substituted DCC molecule for the zero and various applied Electric fields.

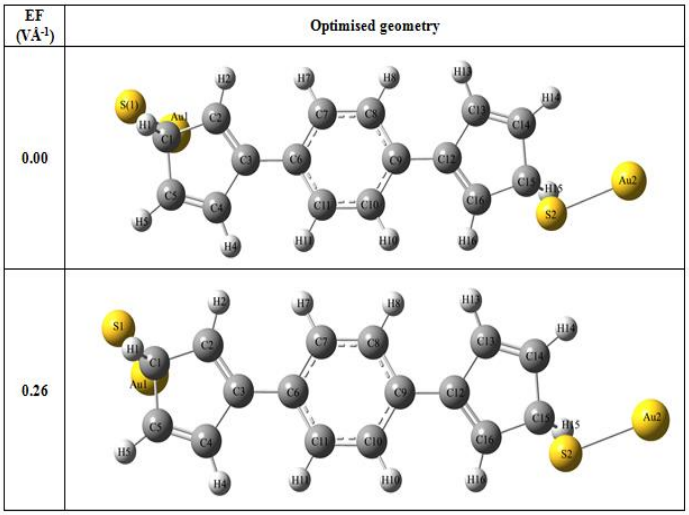

Figure 2. Geometry minimized structure of Au and S substituted DCC molecular wire for the zero and 0.26 VÅ^{-1} Electric fields

The applied field does not appreciably alter the bond angles of the molecule and is almost equal to the predicted angles for the zero field. However, the field made a significant variation in the bond angles of the terminal (S−C−C and Au−S−C) bonds. Precisely, for the zero field, the C−C-S bond angle is ~111.94 and 102° respectively. Further the field increases from 0ev, the S−C−C and Au−S−C bond angles are found to be varied and the maximum angle is found at 0.26 ev. However, the zero field C−C−C bond angles at cyclopentane rings are (~ 109.77°), almost remains the same with the increase of field and for cyclohexane it is observed to be (121.2) which also remains same with the increase of the field.

The applied field made an appreciable increase in the torsion angle of the C−C−C−C bonds of the rings as well as the backbone bonds of the molecule; the maximum difference of torsion angle between zero and the applied field is 0.6°. For the zero field, the torsion angles S–C–C–C bonds in the right end is ~118.9° and the L-end shows the angle of ~126.8°; increase in field shows decrease in angle of variation ~0.1 While Au–S–C–C bonds in the left end shows an appreciable increase when compared with the right end as the field increases; The zero field torsion angle of Au–S–C–C bond is 60.1°; as the field increases, this angle gradually increases with the increase of field (0.26VÅ^{-1}), the terminal bond at the L-end rotates to large extent, the corresponding twist angle is 73.6°; whereas, at the R-end not much variation is noticed.

Overall, when compared with the R-end, the variation in the terminal group of the L-end has been varied significantly, which indicates that this group is highly sensitive to the positive field than the negative field. The structural comparison on various field reveals that, relatively, the terminal groups are found very sensitive to the EF.

Charge density distribution

The application of QTAIM (Quantum theory of atoms in molecules) were made to analyse the chemical nature and electron density at bcp for the Au and Thiol substituted DCC molecule in the present study and the bond topological parameters were tabulated. Table 4 shows the bond topological parameters of DCC molecule for zero and increasing applied Electric fields. The bond topological analysis found a (3,-1) type of bond critical point (bcp) for all bonds of the DCC molecule, detects the mode of chemical bond between two atoms. In the Au and thiol substituted DCC, the interaction between Au and S were found to be weak ionic. The value exhibits by the Laplacian of electron density reveals the nature of the bond, where the positive value shows an ionic interaction (Closed shell [13]) and the negative shows a covalent interaction (Open shell [14]).

Figure 3 displays the complete deformation density of the molecule for the zero and various applied Electric fields, obtained from the difference of total aspherical and spherical atom densities. The deformation density map shows the charge accumulation for the zero and applied fields and the differences. The zero field electron density [$\rho_{bcp}(r)$] at the bcp of all cyclopentyl C−C bonds ranges from 1.60 to 2.10 eÅ^{-3}; when compared with the applied field these values have been slightly reduced and the maximum variation is 0.04 eÅ^{-3}. The average electron density [$\rho_{bcp}(r)$] at the bcp of all cyclohexane C−C bonds are 1.90 eÅ^{-3} and found no significant variation for the applied field. The zero field density $\rho_{bcp}(r)$ of C=C bonds (links the rings) is ~1.73 eÅ^{-3}; the bond densities are found to be almost equal for all the applied fields. The S−C bond density for the zero field is 0.853 eÅ^{-3}, and for the applied field, it slightly increased by maximum of 0.006 eÅ^{-3}.

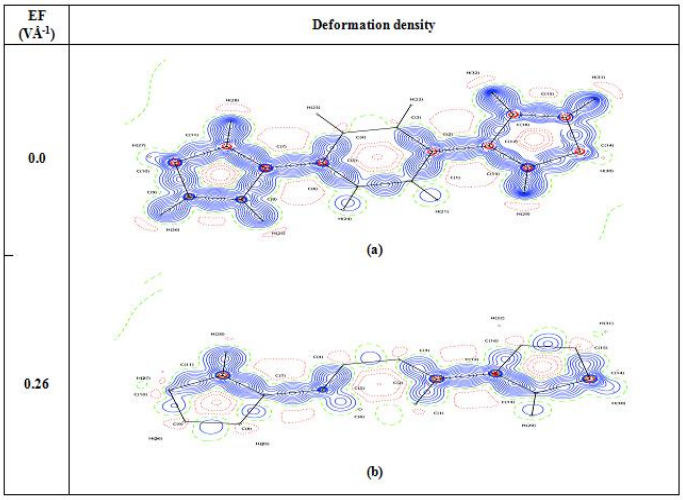

Figure 3. Deformation density plots of Au and S substituted DCC for the (a) zero and (b) 0.26 (VÅ^{-1}) Electric fields. Solid lines represent positive contours, dotted lines are negative contours and dashed lines are zero contours. The contours are drawn at intervals 0.05 eÅ^{-3}

Notably, the S−C bond density is small, which indicates that the charges of these bonds move away from the inter-nuclear axis, which confirms its dominant π-bond nature [14]. This can be well understood from the Laplacian of electron density and the bond ellipticity. The Au−S bond density at zero field is ~0.534 eÅ^{-3}, whereas for the applied field, the variation is found to be very small in both L-end when compared with R-end of the molecule. For the zero field, the C−H bond density is ~1.8 eÅ^{-3}, which is almost equal as the field increases Table 4. The effect of electric field in the DCC molecule did not obviously alter the bond densities of the molecule. The complete $\rho_{bcp}(r)$ values of Au and S substituted DCC molecule for the zero and various applied Electric fields (VÅ^{-1}) are given in Table 4.

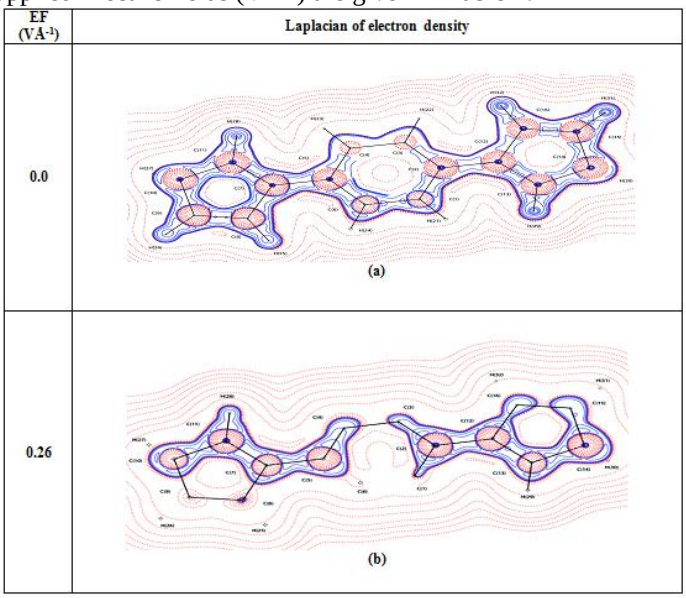

Figure 4. Laplacian of electron density maps of DCC molecule for the (a) zero and (b) 0.26 VÅ^{-1}Electric fields. The contours are drawn in logarithmic scale, 3x2^n eÅ^{-5}, where N = 2, 4 and 8x10^n, n= -2, -1, 0, 1, 2. Solid lines are positive contours and dotted lines are negative contours

Figure 4 shows the Laplacian of electron density for the zero and various applied Electric fields (VÅ^{-1}). For the zero field, the predicted Laplacian of electron density for the cyclohexane C−C bonds are ~ -17.8 eÅ^{-5}; when the field is applied, these values are become little less negative, indicates, the charges of these bonds are slightly depleted. For the cyclopentyl rings, the $\nabla^2\rho_{bcp}(r)$ values of C-C bonds at zero field ranges from -11.9 to 20.8 eÅ^{-5} and there is no significant variation for the increased fields. Similar trend also found in the C=C (links the rings) of the DCC, where the Laplacian for zero field is ~-14.6 eÅ^{-5}; for the applied field, these values were slightly increased by the maximum of 0.4 eÅ^{-5}. For the zero field, the Laplacian for C−H bonds ranges from -19.1 to -20.8 eÅ^{-5}, the high negative value of Laplacian indicates, the charges of the bonds are highly concentrated, whereas for the applied field these values are altered and the maximum variation is 0.4 eÅ^{-5}. The S−C bond charges are less concentrated for the zero field, its corresponding Laplacian is ~ -1.90 eÅ^{-5}; as the field increases, at the L-end the value increases to ~ -2.04 eÅ^{-5} and at the R-end it becomes ~-1.80 eÅ^{-5}; the difference indicates that the charges at the L-end are slightly concentrated than at the R-end. For the zero field, the Laplacian of Au−S bond is ~2.94 eÅ^{-5}, when the field increases, this value increases sharply at the L-end (3.07 eÅ^{-5}) and the trend at the R-end slightly decreases (2.85 eÅ^{-5}). However, the zero field Laplacian of C−H bonds (~ -20.3 eÅ^{-5}), vary slightly with the increase of field. Over all, the Laplacian of electron density distribution in Au−S−DCC−S−Au, reveals that the applied field depletes the charges at the bcps of C−C and C=C bonds, whereas this effect is found little more in the terminal bonds, specifically it is high at the L-end. The calculated Laplacian of electron density values of Au and S substituted DCC molecule for zero and various applied fields are given in Table 5.

The isotropic or anisoatropic nature of electron density distribution at the bcp of molecules can be calculated from the parameter of bond ellipticity $\varepsilon = (\lambda_1/\lambda_2)-1$, where λ_1, λ_2 are the negative eigen values of Hessian matrix. An increased ellipticity value implies deviation from σ-type bond characteristics and also large anisotropy of bonding density. The ellipticity (ε) for cyclohexane C−C bonds [0.13] is found little less when compared with that of cyclopentyl rings and the values are around 0.12. As the field increases, the bond ellipticity of C−C bond at connection part also increases gradually from 0.056 to 0.068. As the field increases, the bond ellipticity of S−C bond at L-end also increases gradually from 0.08 to 0.083, and at the R-end the value decreases from 0.097 to 0.090. In the case of Au−S bonds, the ε is much higher [~0.1] for the increase of field and shows that the densities are found to be highly anisotropic. The deatailed tabulated values for the molecules is represented in Table 6.

Energy density

In order to understand the chemical bonding between the atoms, it should be mandatory to analyse the total energy associated with the bonds. Therefore, the energy density distribution and ESP studies of DCC molecule has been calculated, which is directly related to Laplacian of electron density**.** The total energy density associated with the bond is related as the sum of the potetial energy density V(**r**) and the loal kinetic energy density G(r); H(**r**) = G(**r**) + V(**r**). As noted before, the total energy density is a function of lapacian of electron density. The positive lapacian indicates the dominancy of kinetic energy density and the depletion of bond charge whereas the negative shows that potential energy is dominant by the accumulation of electrons at bcp [15].

Relatively, the predicted zero field energy density H(**r**) for the C−C bonds of cyclohexane ring is high (~-1.862 HÅ^{-3}) when compared with the other bonds in the molecule; as the field increases this value slightly decreases to ~ -1.848 HÅ^{-3}. When the field increases, similar trend persists in the cyclopentyl ring

C–C and in C–H bonds, where the energy densities are -1.674 and 1.713 HÅ^{-3} respectively. The magnitude of the local energy density of Au–S and S–C bonds are significantly less when compared with all other bonds in the molecule. However, the small values are attributed to the nature of bonds; for the applied field, the variation between both types of bonds is found to be opposite. For the applied field, the density H(**r**) of Au–S and S–C bonds are vary from -0.143 to -0.165 HÅ^{-3} and -0.393 to -0.417 HÅ^{-3} respectively. The complete values of energy density distribution of the molecule for various applied Electric fields are listed in Table 7.

Atomic charges

The accumulation of point charges is the key factor which decides the reactivity, intermolecular interaction and the electrostatic potential surface of the concerned molecule [16]. In the current studies the atomic charges were calculated by the use of Mullikan Population Analysis which calculate the atomic charges from the valance level whereas Natural Population Analysis gives more accurate value since the effect of core electrons are being considered. The use of MK (Merz-kollman) method is also highly suggested since it describe the electrostatic interaction more precisely [17]. Hence, in this study, a comparison between NPA and MPA were made to calculate the atomic charges and tabulated in Table 8.

The MPA/NPA charges of all C-atoms except that are linked to S atoms possess negative charge and vary with the increase of field. The linker S(1)-atom possesses a negative NPA/MPA charge, which increases from -0.513 to -0.532e and with the increase of field, while the charge of S(2)-atom increases from -0.351 to -0.363e. As the field increases, the NPA charges of Au atom at L-end increases from 0.246 to 0.253e, but the same at R-end decreases from 0.182 to 0.035e. For the zero field, the MPA charge for all C-atoms are found almost negative, and the H-atoms are positive; when the field increases, the charges also increases. For the applied field, the MPA charge of S-atom at the L-end increases gradually from 0.052 to 0.1e, while at the R-end this effect is opposite and increases from 0.046 to 0.052e. As the field increases, the charges of Au(1) atom increases from 0.246 to 0.253e, but the same for Au(2) decreases from 0.182 to 0.035e. Table 8 shows the difference of charge distribution for zero and various applied Electric fields.

Molecular orbital analysis

The energy gap between the the Highest occupied molecular orbital and the Lowest unoccupied molecular orbital is called as the HLG (Homo Lumo Energy Gap). This Energy gap plays a vital role in many physical, chemical and semiconducting properties of the molecules [18,19], so the variation of the HLG with the applied field is very much necessary to examine. Figure 5 shows the HOMO LUMO distribution of Au and Thiol substituted DCC for 0.0 and 0.26 VÅ^{-1}, and is clearly observed that the reverse field localized the molecule in a manner which is symmetric and opposite to each other. For the applied field (0.00 - 0.26 VÅ^{-1}), the HLG decreases from 2.09 to 0.71 eV.

Figure 6 illustrates the density of states (DOS) for the zero and maximum applied field (0.26 VÅ^{-1}), in which the green lines indicate the HOMO and the blue is LUMO; the decrease of HLG is also shown. Here, the hybridization of the molecular level with that of the gold atom broadens the DOS peaks. At 0.05 VÅ^{-1}, the DOS peaks are in minima, indicates the discrete molecular level with HLG, 1.44 eV, further increase of field from 0.10 to 0.26 VÅ^{-1}, both HOMO and LUMO levels approach each other and their gap decreases notably from 1.14 to 0.71 eV.

The plot between the HLG and the Electric fields shows the decrease of the band gap energy between HOMO and LUMO, which implies the increase in conduction thought the Au and Thiol substiued DCC nano wire [20]. Thus it can be stated as the increase of applied electric field may increase the conductivity in a most linear way, and the Au and thiol substituted DCC molecule can act as an efficient molecular nanowire. Figure 7 illustrates the energy levels of the molecule for zero and 0.26 VÅ^{-1} Electric fields.

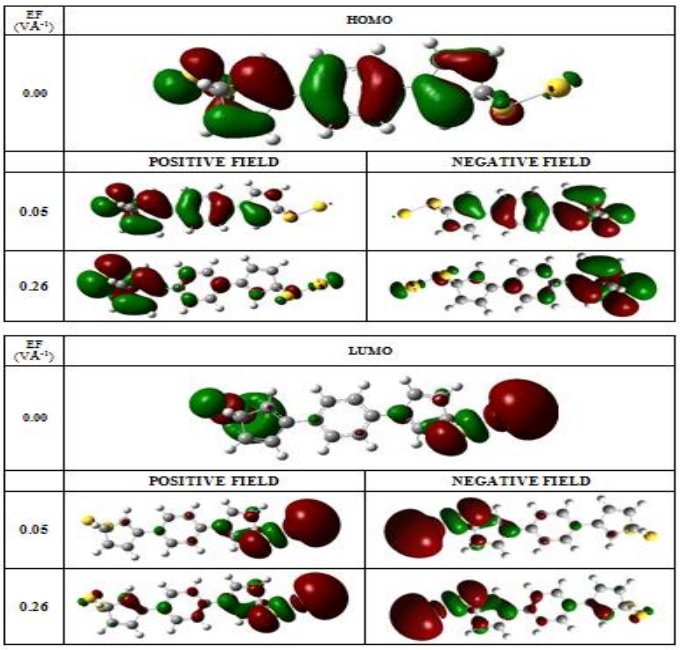

Figure 5. HOMO and LUMO surface representation of molecular orbitals of Au and S substituted DCC for the zero and 0.26 VÅ^{-1} EF, which are drawn at 0.05 au surface values

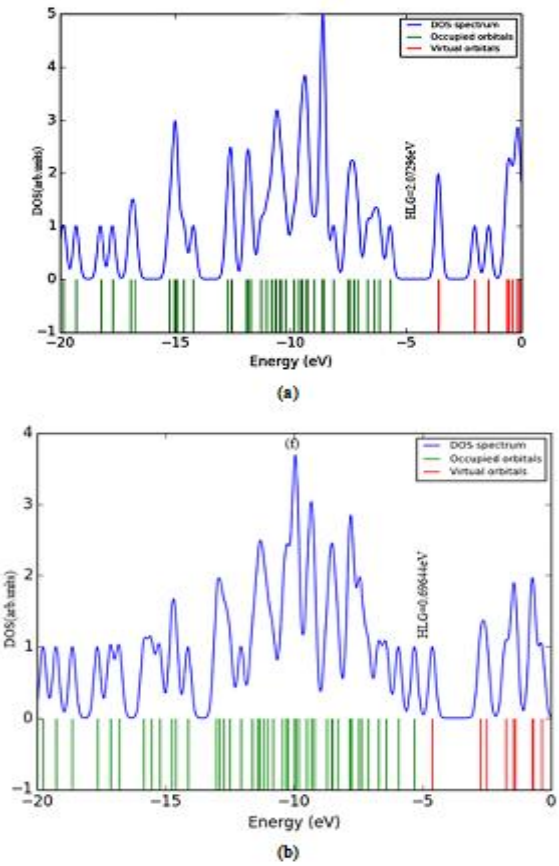

Figure 6(a b). DOS of Au and S substituted DCC for the (a) zero and (b) 0.26 VÅ^{-1}Electric fields

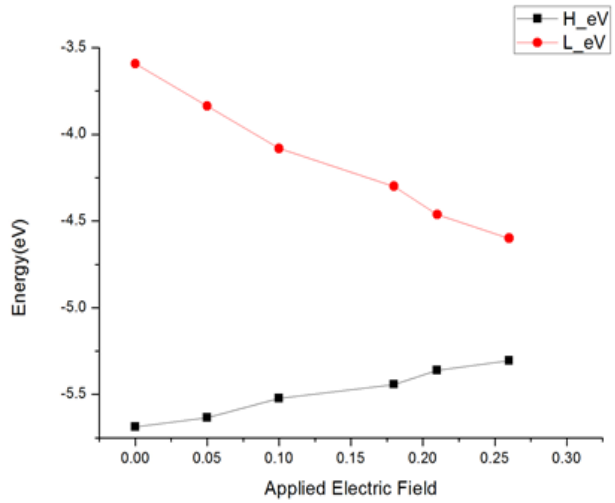

Figure 7. Variation of HLG of Au and S substituted DCC for the zero and various applied Electric fields

Electrostatic potential

The positively and negatively charged regions of the DCC molecule is identified from the electrostatic potential (ESP) surface of the molecule [21,22]. Analysing a ESP surface will give the idea about the reactive surface of the concerned molecule. Figure 8 is the iso surface representation of ESP of DCC molecule, in which the Au–S bond regions exhibit high negative ESP. The Electrostatic Potential Surface map [23] clearly shows the charged regions of the molecule, and it shows the effect of nuclei and the electrons in the negative as well as positivly charged regions. For the zero bias, the negative ESP is concentrated around the S-atoms, which are present at either ends of the molecule, and the rest of the molecule carries positive ESP. For the increase of positive field from 0 to 0.15 $VÅ^{-1}$, the negative ESP at the L-end decreases for each biasing step and it disappears, while at the R-end, the negative ESP increases and spread around the right edge of the molecule. Further, increase of field to 0.26 $VÅ^{-1}$, the negative ESP spread entirely around the R-end of the molecule, which indicates that as the field increases the charge seems to drift from left to right. Similarly, when the field is reversed the negative ESP regions are moved from R-end to L-end of the molecule.

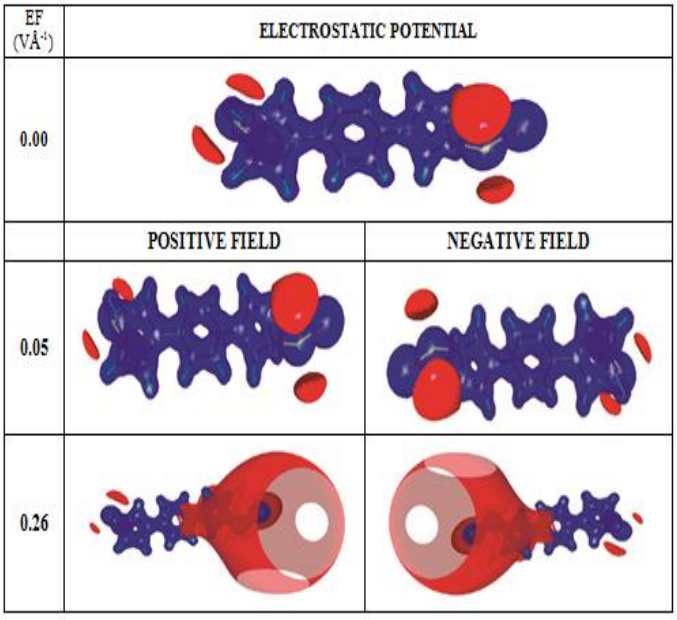

Figure 8. Electrostatic potentials of Au and S substituted DCC for the zero and 0.26 $VÅ^{-1}$ Electric fields. Blue: (0.5 $eÅ^{-1}$) positive potential Red: (-0.04 $eÅ^{-1}$) negative potential

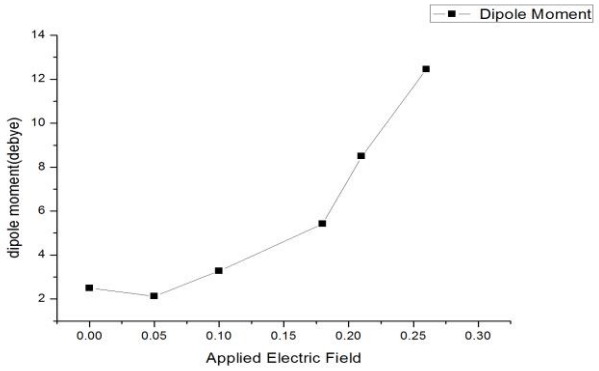

Figure 9. Variation of molecular dipole moment of Au and S substituted DCC for various applied Electric fields

Molecular dipole moment

The applied electric field may alter the polarity of the molecule, which obviously affect the dipole moment associated with it. The work by Kirtman et al., [24] made a study on the variations of molecular dipole moment with the electric field, and it showed a linearity in the variations which extends upto certain voltage and the same disappears at high voltage. The variation of molecular dipole moment for various applied Electric fields is shown in Figure 9. The molecular dipole moment for zero bias is 2.50 debye, which increases almost linearly with the increase of field. The molecule becomes highly polarized for the higher field (0.26 $VÅ^{-1}$); the polarization induces to have high molecular dipole moment value of 12.45 debye. However, further increasing the applied field, the "high voltage" may regime to warrant nonlinear variations in the electric dipole moment as reported by Rai *et al* [25].

I–V characteristic curve

The relation of Current with Voltage is the vital parameter which governs almost all electronic devices as well as the conducting and semiconducting molecules. The plot between the current and the voltage is called as the IV characteristics curve[26]. In the present study, the I-V characteristics of the DCC molecule have been evaluated using the Landauer formula [27]. The tunneling electric current (I) has been calculated for various applied Electric fields. The resistance (R) and the linear conductance (G) of the electrode–molecule–electrode junctions can be expressed as

$$R = G^{-1} = (h/2e^2)\,(1/\,T_l T_r T_m) = (12.91\ K\Omega)/\,T_l T_r T_m \qquad (1)$$

The calculated resistance is used to find the the tunneling current I, from the relation between I, V and R. For an applied field V can be expressed as EL, where L is the geometric length of the molecule between the two terminals [28,29].

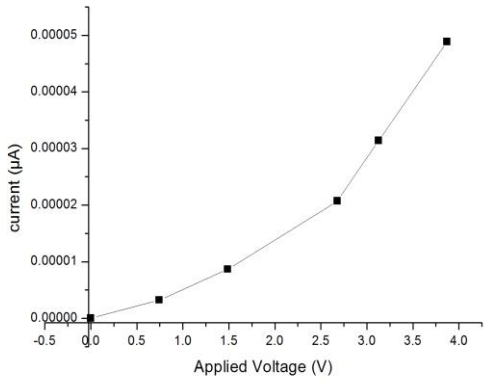

Figure 10. I-V characteristics curve of DCC molecule for different applied Electric fields

Table 1. Bond lengths (Å) of Au and S substituted DCC molecule for the zero and different applied Electric fields (VÅ^{-1})

Bonds		Applied Electric Field (VÅ^{-1})				
	0	0.05	0.10	0.18	0.21	0.28
Ring 1						
C(3)−C(2)	1.3717	1.3717	1.3721	1.373	1.3747	1.3772
C(3)−C(4)	1.4933	1.4928	1.4923	1.4917	1.4909	1.4895
C(2)−C(1)	1.5082	1.5079	1.5074	1.5067	1.5054	1.5042
C(1)−C(5)	1.5138	1.5135	1.5131	1.5127	1.5122	1.5116
C(5)−C(4)	1.3597	1.3599	1.3601	1.3604	1.361	1.3618
Ring 2						
C(7)−C(6)	1.4174	1.4178	1.4184	1.4193	1.4206	1.4218
C(6)−C(11)	1.4184	1.4188	1.4194	1.4203	1.4215	1.4228
C(10)−C(9)	1.4167	1.4169	1.4174	1.4182	1.4192	1.4205
C(9)−C(8)	1.4186	1.4188	1.4194	1.4202	1.4214	1.4225
Ring 3						
C(12)−C(13)	1.4891	1.4891	1.489	1.4889	1.4887	1.4886
C(12)−C(16)	1.3752	1.3764	1.3781	1.3803	1.3827	1.385
C(13)−C(14)	1.3599	1.3599	1.3599	1.36	1.3601	1.3603
C(14)−C(15)	1.5112	1.5113	1.5113	1.5112	1.511	1.5109
C(15)−C(16)	1.5087	1.5083	1.5077	1.5068	1.5058	1.5051
Ring Connectors						
C(6)−C(3)	1.4749	1.4745	1.4737	1.4725	1.4707	1.4686
C(9)−C(12)	1.4735	1.4725	1.471	1.469	1.4665	1.4645
Terminal						
C(15)−S(2)	1.9353	1.9345	1.9337	1.9327	1.9317	1.9308
C(1)−S(1)	1.9252	1.924	1.9231	1.9225	1.9233	1.9238
S(2)−Au(2)	2.3909	2.3938	2.398	2.4045	2.4142	2.427
S(1)−Au(1)	2.3851	2.3848	2.3846	2.3843	2.3855	2.3856
C−H Bonds						
C(1)−H(1)	1.101	1.101	1.101	1.101	1.101	1.101
C(2)−H(2)	1.083	1.083	1.083	1.083	1.083	1.083
C(4)−H(4)	1.084	1.084	1.084	1.084	1.084	1.084
C(5)−H(5)	1.083	1.083	1.083	1.083	1.083	1.083
C(7)−H(7)	1.087	1.087	1.087	1.086	1.086	1.086
C(10)−H(10)	1.087	1.087	1.087	1.087	1.087	1.087
C(8)−H(8)	1.087	1.087	1.087	1.087	1.087	1.087
C(13)−H(13)	1.084	1.084	1.084	1.084	1.084	1.084
C(14)−H(14)	1.083	1.084	1.084	1.084	1.084	1.084
C(15)−H(15)	1.094	1.0938	1.0937	1.0935	1.0934	1.0934
C(16)−H(16)	1.083	1.083	1.083	1.083	1.083	1.083

Table 2. Bond angles (°) of Au and S substituted DCC molecule for the zero and different applied Electric fields (VÅ^{-1})

Bonds	Applied Electric Field (VÅ^{-1})					
	0	0.05	0.10	0.18	0.21	0.26
Ring 1 C(2)−C(3)−C(4)	107.9	107.9	107.9	107.9	107.8	107.8
C(3)−C(2)−C(1)	109.8	109.7	109.7	109.7	109.8	109.8
C(2)−C(1)−C(5)	103.6	103.6	103.6	103.6	103.6	103.6
C(1)−C(5)−C(4)	108.9	108.9	109.0	109.0	109.0	109.1
C(3)−C(4)−C(5)	109.8	109.8	109.7	109.7	109.7	109.7
Ring 2						
C(6)−C(7)−C(8)	121.3	121.3	121.3	121.3	121.4	121.4
C(7)−C(6)−C(11)	117.4	117.4	117.4	117.4	117.3	117.2
C(7)−C(6)−C(3)	121.4	121.4	121.4	121.4	121.4	121.5
C(11)−C(6)−C(3)	121.1	121.1	121.2	121.2	121.3	121.3
C(6)−C(11)−C(10)	121.3	121.3	121.3	121.3	121.4	121.4
C(11)−C(10)−C(9)	121.2	121.2	121.2	121.2	121.2	121.3
C(10)−C(9)−C(8)	117.5	117.5	117.5	117.5	117.4	117.4
C(7)−C(8)−C(9)	121.3	121.2	121.3	121.3	121.3	121.3
Ring 3						
C(13)−C(12)−C(16)	108.0	107.9	107.9	107.8	107.7	107.6
C(12)−C(13)−C(14)	109.7	109.7	109.8	109.8	109.8	109.9
C(13)−C(14)−C(15)	109.2	109.2	109.2	109.2	109.2	109.2
C(14)−C(15)−C(16)	103.5	103.5	103.5	103.6	103.6	103.6
C(12)−C(16)−C(15)	109.6	109.6	109.7	109.7	109.7	109.7
Ring Connectors						
C(6)−C(3)−C(2)	127.6	127.5	127.3	127.2	127.0	126.8
C(6)−C(3)−C(4)	124.5	124.6	124.7	124.9	125.2	125.4
C(10)−C(9)−C(12)	121.4	121.4	121.5	121.5	121.6	121.7

C(8)−C(9)−C(12)	121.1	121.0	121.0	121.0	121.0	120.9
C(9)−C(12)−C(13)	124.5	124.5	124.4	124.4	124.4	124.4
C(9)−C(12)−C(16)	127.5	127.6	127.7	127.8	127.9	127.9
Terminal						
C(14)−C(15)−S(2)	112.7	112.6	112.4	112.3	112.3	112.3
C(16)−C(15)−S(2)	106.1	105.8	105.4	104.9	104.4	104.2
C(2)−C(1)−S(1)	114.6	114.5	114.3	114.1	113.6	113.1
C(5)−C(1)−S(1)	114.4	114.6	114.8	115.0	115.3	115.4
C(15)−S(2)−Au(2)	102.8	102.9	103.1	103.4	103.8	104.1
C(1)−S(1)−Au(1)	101.2	101.6	101.9	102.3	102.6	103.0

Table 3. Torsion angles (°) of Au and S substituted DCC for the zero and different applied Electric fields (VÅ^{-1})

Bonds	**Applied Electric Field (VÅ^{-1})**					
	0	**0.05**	**0.10**	**0.18**	**0.21**	**0.26**
Ring 1 C(4)−C(3)−C(2)−C(1)	0.6	0.6	0.5	0.5	0.5	0.4
C(2)−C(3)−C(4)−C(5)	0.3	0.3	0.3	0.4	0.3	0.3
C(3)−C(2)−C(1)−C(5)	-1.1	-1.1	-1.1	-1.1	-1.0	-0.9
C(2)−C(1)−C(5)−C(4)	1.3	1.3	1.3	1.3	1.2	1.1
C(1)−C(5)−C(4)−C(3)	-1.0	-1.0	-1.1	-1.1	-0.9	-0.9
C(6)−C(3)−C(2)−C(1)	-179.5	-179.5	-179.4	-179.3	-179.1	-178.9
C(6)−C(3)−C(4)−C(5)	-179.7	-179.7	-179.7	-179.8	179.9	179.7
Ring 2						
C(8)−C(7)−C(6)−C(11)	-0.4	-0.4	-0.4	-0.4	-0.4	-0.2
C(8)−C(7)−C(6)−C(3)	179.0	179.0	179.1	179.1	179.1	179.1
C(6)−C(7)−C(8)−C(9)	0.4	0.5	0.5	0.5	0.5	0.5
C(7)−C(6)−C(11)−C(10)	0.4	0.3	0.3	0.2	0.1	0.0
C(3)−C(6)−C(11)−C(10)	-179.1	-179.1	-179.2	-179.2	-179.3	-179.4
C(10)−C(9)−C(8)−C(7)	-0.3	-0.3	-0.4	-0.4	-0.4	-0.5
C(6)−C(11)−C(10)−C(9)	-0.3	-0.3	-0.2	-0.2	-0.1	0.0
C(11)−C(10)−C(9)−C(8)	0.3	0.2	0.2	0.2	0.2	0.2
Ring 3						
C(13)−C(12)−C(16)−C(15)	0.3	0.2	0.2	0.1	0.0	-0.2
C(12)−C(13)−C(14)−C(15)	0.8	0.8	0.8	0.8	0.7	0.7
C(13)−C(14)−C(15)−C(16)	-0.6	-0.7	-0.7	-0.7	-0.7	-0.8
C(16)−C(12)−C(13)−C(14)	-0.7	-0.7	-0.6	-0.5	-0.4	-0.3
Ring Connectors						
C(7)−C(6)−C(3)−C(2)	-14.4	-14.8	-14.9	-14.5	-12.0	-11.6
C(7)−C(6)−C(3)−C(4)	165.5	165.1	165.1	165.7	168.4	169.1
C(11)−C(6)−C(3)−C(2)	165.0	164.6	164.6	165.0	167.4	167.7
C(11)−C(6)−C(3)−C(4)	-15.1	-15.4	-15.4	-14.8	-12.2	-11.5
C(11)−C(10)−C(9)−C(12)	-179.7	-179.6	-179.4	-179.3	-179.1	-178.8
C(12)−C(9)−C(8)−C(7)	179.6	179.5	179.3	179.1	178.9	178.6
C(10)−C(9)−C(12)−C(13)	-162.2	-162.6	-163.4	-164.4	-164.9	-165.9
C(10)−C(9)−C(12)−C(16)	18.5	18.2	17.8	17.2	17.0	16.6
C(8)−C(9)−C(12)−C(13)	17.9	17.6	17.0	16.2	15.8	15.1
C(8)−C(9)−C(12)−C(16)	-161.5	-161.6	-161.9	-162.3	-162.2	-162.4
C(9)−C(12)−C(13)−C(14)	179.8	-180.0	-179.6	-179.3	-178.8	-178.2
C(9)−C(12)−C(13)−H(13)	2.4	2.7	3.0	3.4	4.0	4.6
C(9)−C(12)−C(16)−C(15)	179.8	179.5	179.1	178.8	178.2	177.6
Terminal						
C(13)−C(14)−C(15)−S(2)	-114.7	-114.4	-113.9	-113.3	-112.8	-112.6
C(14)−C(15)−C(16)−C(12)	0.1	0.2	0.3	0.3	0.4	0.6
S(2)−C(15)−C(16)−C(12)	118.9	118.8	118.5	118.3	118.1	118.2
C(14)−C(15)−S(2)−Au(2)	-66.9	-66.4	-66.2	-66.3	-66.6	-67.1
C(16)−C(15)−S(2)−Au(2)	-179.4	-178.7	-178.3	-178.1	-178.2	-178.5
C(3)−C(2)−C(1)−S(1)	-126.5	-126.6	-126.8	-126.9	-126.8	-126.5
S(1)−C(1)−C(5)−C(4)	126.8	126.7	126.7	126.6	125.9	125.2
C(2)−C(1)−S(1)−Au(1)	60.1	61.6	63.1	65.3	71.3	73.6
C(5)−C(1)−S(1)−Au(1)	-59.4	-58.0	-56.5	-54.3	-48.0	-45.4

Table 4. Electron density $\rho_{bcp}(r)$ ($eÅ^{-3}$) values of Au and S substituted DCC for the zero and different applied Electric Fields ($VÅ^{-1}$)

Bonds	Applied Electric Field($VÅ^{-1}$)					
	0	**0.05**	**0.10**	**0.18**	**0.21**	**0.26**
Ring 1 C(3)−C(2)	2.06	2.06	2.06	2.06	2.05	2.04
C(3)−C(4)	1.65	1.65	1.65	1.65	1.66	1.66
C(2)−C(1)	1.62	1.62	1.62	1.62	1.63	1.63
C(1)−C(5)	1.60	1.60	1.60	1.60	1.60	1.60
C(5)−C(4)	2.10	2.10	2.10	2.10	2.10	2.09
Ring 2						
C(7)−C(6)	1.90	1.90	1.90	1.90	1.89	1.89
C(7)−C(8)	1.96	1.96	1.96	1.97	1.97	1.97
C(6)−C(11)	1.90	1.90	1.90	1.89	1.89	1.89
C(10)−C(9)	1.90	1.90	1.90	1.90	1.89	1.89
C(9)−C(8)	1.90	1.90	1.89	1.89	1.89	1.88
C(8)−H(8)	1.79	1.79	1.79	1.79	1.79	1.79
Ring 3						
C(12)−C(13)	1.67	1.67	1.67	1.67	1.67	1.67
C(12)−C(16)	2.05	2.04	2.04	2.03	2.02	2.01
C(13)−C(14)	2.10	2.10	2.10	2.10	2.10	2.10
C(14)−C(15)	1.61	1.61	1.61	1.61	1.61	1.61
C(15)−C(16)	1.61	1.61	1.61	1.61	1.61	1.62
Ring Connectors						
C(6)−C(3)	1.71	1.71	1.72	1.72	1.73	1.73
C(9)−C(12)	1.72	1.72	1.73	1.73	1.74	1.75
Terminal						
C(15)−S(2)	0.844	0.846	0.847	0.848	0.849	0.85
C(1)−S(1)	0.862	0.864	0.865	0.865	0.862	0.861
S(2)−Au(2)	0.53	0.526	0.522	0.515	0.506	0.494
S(1)−Au(1)	0.537	0.537	0.537	0.537	0.536	0.536
C−H Bonds						
H(1)−C(1)	1.72	1.72	1.72	1.72	1.72	1.72
C(2)−H(2)	1.79	1.79	1.79	1.80	1.80	1.80
C(4)−H(4)	1.79	1.79	1.79	1.79	1.79	1.79
C(5)−H(5)	1.80	1.80	1.80	1.80	1.80	1.81
C(7)−H(7)	1.79	1.79	1.79	1.80	1.80	1.80
C(10)−H(10)	1.79	1.79	1.79	1.79	1.79	1.79
C(11)−H(11)	1.79	1.79	1.80	1.80	1.80	1.80
C(13)−H(13)	1.79	1.79	1.79	1.80	1.80	1.80
C(14)−H(14)	1.79	1.79	1.79	1.79	1.79	1.79
C(15)−H(15)	1.761	1.762	1.763	1.764	1.764	1.763
C(16)−H(16)	1.79	1.79	1.79	1.79	1.79	1.79

Table 5. Laplacian of electron density $\nabla^2\rho_{bcp}(r)$ ($eÅ^{-5}$) values of Au and S substituted DCC for the zero and different applied Electric fields ($VÅ^{-1}$)

Bonds	Applied electric field ($VÅ^{-1}$)					
	0	**0.05**	**0.10**	**0.18**	**0.21**	**0.26**
Ring 1 C(3)−C(2)	-20.0	-20.0	-20.0	-19.9	-19.9	-19.7
C(3)−C(4)	-13.0	-13.0	-13.0	-13.0	-13.1	-13.1
C(2)−C(1)	-12.2	-12.3	-12.3	-12.4	-12.5	-12.6
C(1)−C(5)	-11.9	-12.0	-12.0	-12.0	-12.0	-12.1
C(5)−C(4)	-20.8	-20.7	-20.7	-20.7	-20.7	-20.7
Ring 2						
C(7)−C(6)	-17.6	-17.6	-17.6	-17.5	-17.5	-17.4
C(7)−C(8)	-18.7	-18.7	-18.7	-18.8	-18.9	-18.9
C(6)−C(11)	-17.5	-17.5	-17.5	-17.5	-17.4	-17.4
C(10)−C(9)	-17.6	-17.6	-17.6	-17.5	-17.5	-18.8
C(9)−C(8)	-17.5	-17.5	-17.4	-17.4	-17.3	-17.3
Ring 3						
C(12)−C(13)	-13.2	-13.3	-13.3	-13.3	-13.3	-13.4
C(12)−C(16)	-19.8	-19.7	-19.6	-19.5	-19.3	-19.2
C(13)−C(14)	-20.8	-20.8	-20.8	-20.8	-20.8	-20.8
C(14)−C(15)	-12.1	-12.1	-12.1	-12.1	-12.1	-12.1
C(15)−C(16)	-12.1	-12.1	-12.1	-12.2	-12.2	-12.3
Ring Connectors						
C(6)−C(3)	-14.5	-14.6	-14.6	-14.7	-14.8	-14.9
C(9)−C(12)	-14.7	-14.7	-14.8	-14.9	-15.0	-15.1

Terminal						
C(15)−S(2)	-1.806	-1.806	-1.804	-1.8	-1.797	-1.798
C(1)−S(1)	-2.007	-2.03	-2.046	-2.056	-2.037	-2.019
S(2)−Au(2)	2.898	2.868	2.846	2.834	2.836	2.851
S(1)−Au(1)	2.988	2.99	2.996	3.009	3.035	3.074
C−H Bonds						
H(1)−C(1)	-19.1	-18.7	-18.8	-18.8	-18.9	-19.1
C(2)−H(2)	-20.6	-20.6	-20.7	-20.7	-20.8	-20.9
C(4)−H(4)	-20.5	-20.5	-20.4	-20.4	-20.4	-20.4
C(5)−H(5)	-20.8	-20.9	-21.0	-21.1	-21.2	-21.4
C(7)−H(7)	-20.3	-20.4	-20.5	-20.5	-20.6	-20.7
C(8)−H(8)	-20.3	-20.3	-20.2	-20.2	-20.2	-20.2
C(10)−H(10)	-20.4	-20.3	-20.3	-20.3	-20.2	-20.2
C(11)−H(11)	-20.3	-20.4	-20.4	-20.5	-20.6	-20.6
C(13)−H(13)	-20.5	-20.6	-20.7	-20.7	-20.8	-20.8
C(14)−H(14)	-20.7	-20.7	-20.6	-20.6	-20.6	-20.5
C(15)−H(15)	-19.811	-19.808	-19.805	-19.801	-19.785	-19.742
C(16)−H(16)	-20.5	-20.5	-20.6	-20.6	-20.6	-20.6

Table 6. Bond ellipticity values of Au and S substituted DCC for the zero and different applied Electric fields (VÅ^{-1})

Bonds	**Applied electric field(VÅ^{-1})**					
	0	**0.05**	**0.10**	**0.18**	**0.21**	**0.26**
Ring 1 C(3)−C(2)	0.239	0.237	0.233	0.229	0.221	0.211
C(3)−C(4)	0.058	0.06	0.062	0.064	0.065	0.067
C(2)−C(1)	0.037	0.036	0.036	0.035	0.034	0.033
C(1)−C(5)	0.029	0.029	0.029	0.029	0.029	0.028
C(5)−C(4)	0.248	0.247	0.247	0.246	0.244	0.241
Ring 2						
C(7)−C(6)	0.134	0.132	0.129	0.126	0.122	0.119
C(7)−C(8)	0.153	0.153	0.153	0.154	0.155	0.132
C(6)−C(11)	0.134	0.132	0.129	0.126	0.122	0.119
C(10)−C(9)	0.136	0.137	0.137	0.136	0.134	0.132
C(9)−C(8)	0.134	0.135	0.135	0.134	0.132	0.13
Ring 3						
C(12)−C(13)	0.059	0.057	0.055	0.054	0.053	0.053
C(12)−C(16)	0.231	0.229	0.225	0.22	0.215	0.21
C(13)−C(14)	0.246	0.245	0.244	0.243	0.242	0.241
C(14)−C(15)	0.024	0.023	0.023	0.023	0.022	0.022
C(15)−C(16)	0.037	0.038	0.039	0.039	0.04	0.04
Ring Connectors						
C(6)−C(3)	0.058	0.058	0.058	0.059	0.061	0.063
C(9)−C(12)	0.056	0.058	0.06	0.062	0.065	0.068
Terminal						
C(15)−S(2)	0.097	0.096	0.094	0.093	0.091	0.09
C(1)−S(1)	0.08	0.08	0.082	0.083	0.084	0.083
S(2)−Au(2)	0.101	0.102	0.102	0.103	0.102	0.102
S(1)−Au(1)	0.099	0.099	0.099	0.099	0.098	0.096
C−H Bonds						
C(1)−H(1)	0.007	0.006	0.005	0.004	0.004	0.004
C(2)−H(2)	0.013	0.011	0.009	0.007	0.005	0.004
C(4)−H(4)	0.004	0.005	0.006	0.007	0.007	0.007
C(5)−H(5)	0.008	0.007	0.007	0.006	0.005	0.004
C(7)−H(7)	0.004	0.004	0.004	0.004	0.004	0.004
C(10)−H(10)	0.003	0.003	0.003	0.003	0.002	0.002
C(11)−H(11)	0.004	0.004	0.004	0.004	0.004	0.004
C(13)−H(13)	0.005	0.005	0.004	0.004	0.004	0.004
C(14)−H(14)	0.007	0.007	0.008	0.008	0.008	0.008
C(15)−H(15)	0.007	0.008	0.008	0.009	0.009	0.009
C(16)−H(16)	0.016	0.017	0.018	0.018	0.019	0.019

Table 7. Bond energy density H(r) ($HÅ^{-3}$) values of Au and S substituted DCC molecule for the zero and different applied Electric fields ($VÅ^{-1}$)

Bonds	Applied electric field ($VÅ^{-1}$)					
	0	**0.05**	**0.10**	**0.18**	**0.21**	**0.26**
Ring 1 C(3)−C(2)	-2.17	-2.17	-2.17	-2.16	-2.15	-2.13
C(3)−C(4)	-1.37	-1.37	-1.37	-1.38	-1.38	-1.39
C(2)−C(1)	-1.30	-1.30	-1.31	-1.31	-1.32	-1.33
C(1)−C(5)	-1.27	-1.27	-1.27	-1.28	-1.28	-1.28
C(5)−C(4)	-2.26	-2.26	-2.26	-2.25	-2.25	-2.24
Ring 2						
C(7)−C(6)	-1.84	-1.84	-1.84	-1.83	-1.82	-1.82
C(7)−C(8)	-1.96	-1.96	-1.97	-1.97	-1.98	-1.99
C(6)−C(11)	-1.83	-1.83	-1.83	-1.82	-1.82	-1.81
C(10)−C(9)	-1.85	-1.84	-1.84	-1.83	-1.83	-1.82
C(9)−C(8)	-1.83	-1.83	-1.83	-1.82	-1.81	-1.80
Ring 3						
C(12)−C(13)	-1.39	-1.39	-1.40	-1.40	-1.40	-1.40
C(12)−C(16)	-2.15	-2.14	-2.12	-2.11	-2.09	-2.07
C(13)−C(14)	-2.26	-2.26	-2.26	-2.26	-2.26	-2.26
C(13)−H(13)	-1.73	-1.73	-1.73	-1.74	-1.74	-1.74
C(14)−C(15)	-1.29	-1.28	-1.28	-1.28	-1.29	-1.29
C(14)−H(14)	-1.74	-1.73	-1.73	-1.73	-1.73	-1.73
C(15)−C(16)	-1.29	-1.29	-1.30	-1.30	-1.31	-1.31
Ring Connectors						
C(6)−C(3)	-1.47	-1.47	-1.48	-1.49	-1.50	-1.51
C(9)−C(12)	-1.48	-1.49	-1.50	-1.51	-1.52	-1.54
Terminal						
C(15)−S(2)	-0.393	-0.394	-0.395	-0.395	-0.397	-0.398
C(1)−S(1)	-0.413	-0.415	-0.417	-0.418	-0.417	-0.416
S(2)−Au(2)	-0.163	-0.162	-0.16	-0.155	-0.15	-0.143
S(1)−Au(1)	-0.166	-0.166	-0.166	-0.165	-0.165	-0.165
C−H Bonds						
C(1)−H(1)	-1.60	-1.60	-1.60	-1.60	-1.61	-1.61
C(2)−H(2)	-1.73	-1.74	-1.74	-1.74	-1.74	-1.75
C(4)−H(4)	-1.73	-1.72	-1.72	-1.72	-1.72	-1.73
C(5)−H(5)	-1.74	-1.74	-1.75	-1.75	-1.76	-1.76
C(7)−H(7)	-1.72	-1.72	-1.73	-1.73	-1.73	-1.74
C(10)−H(10)	-1.72	-1.72	-1.72	-1.72	-1.71	-1.71
C(11)−H(11)	-1.72	-1.72	-1.73	-1.73	-1.73	-1.74
C(13)−H(13)	-1.73	-1.73	-1.73	-1.74	-1.74	-1.74
C(14)−H(14)	-1.74	-1.73	-1.73	-1.73	-1.73	-1.73
C(15)−H(15)	-1.68	-1.68	-1.68	-1.68	-1.68	-1.67
C(16)−H(16)	-1.73	-1.73	-1.74	-1.74	-1.74	-1.74

Table 8. Atomic charges (e) of Au and S substituted DCC for the zero and different applied Electric fields ($VÅ^{-1}$)

Atoms	Applied electric field ($VÅ^{-1}$)					
	0	**0.05**	**0.10**	**0.18**	**0.21**	**0.26**
C(1)	-0.513	-0.517	-0.521	-0.526	-0.532	-0.532
	-0.351	-0.354	-0.357	-0.36	-0.363	-0.363
C(2)	-0.348	-0.344	-0.339	-0.333	-0.321	-0.321
	-0.192	-0.184	-0.175	-0.164	-0.149	-0.149
C(3)	0.329	0.328	0.328	0.327	0.326	0.326
	-0.058	-0.062	-0.066	-0.07	-0.073	-0.073
C(4)	-0.335	-0.337	-0.339	-0.34	-0.34	-0.34
	-0.219	-0.223	-0.226	-0.229	-0.231	-0.231
C(5)	-0.197	-0.193	-0.19	-0.185	-0.182	-0.182
	-0.193	-0.189	-0.184	-0.179	-0.175	-0.175
C(6)	0.369	0.37	0.371	0.372	0.373	0.373
	-0.05	-0.043	-0.036	-0.029	-0.022	-0.022
C(7)	-0.39	-0.389	-0.388	-0.386	-0.382	-0.382
	-0.183	-0.183	-0.183	-0.182	-0.18	-0.18
C(8)	-0.381	-0.38	-0.378	-0.376	-0.376	-0.376
	-0.188	-0.187	-0.186	-0.185	-0.184	-0.184
C(9)	0.362	0.362	0.362	0.362	0.364	0.364
	-0.057	-0.062	-0.067	-0.071	-0.073	-0.073
C(10)	-0.389	-0.388	-0.387	-0.386	-0.386	-0.386
	-0.179	-0.178	-0.177	-0.175	-0.174	-0.174
C(11)	-0.381	-0.381	-0.381	-0.381	-0.379	-0.379

	-0.192	-0.192	-0.192	-0.192	-0.191	-0.191
C(12)	0.326	0.327	0.328	0.328	0.327	0.327
	-0.039	-0.033	-0.027	-0.022	-0.019	-0.019
C(13)	-0.353	-0.35	-0.347	-0.344	-0.341	-0.341
	-0.219	-0.215	-0.212	-0.21	-0.208	-0.208
C(14)	-0.136	-0.138	-0.141	-0.145	-0.148	-0.148
	-0.179	-0.181	-0.183	-0.184	-0.184	-0.184
C(15)	-0.486	-0.485	-0.484	-0.484	-0.483	-0.483
	-0.334	-0.332	-0.331	-0.33	-0.329	-0.329
C(16)	-0.392	-0.394	-0.395	-0.395	-0.394	-0.394
	-0.204	-0.209	-0.214	-0.217	-0.218	-0.218
S(2)	0.046	0.05	0.053	0.054	0.052	0.052
	-0.168	-0.16	-0.154	-0.149	-0.148	-0.148
S(1)	0.052	0.064	0.076	0.088	0.1	0.1
	-0.177	-0.167	-0.158	-0.149	-0.142	-0.142
Au(2)	-0.071	-0.098	-0.128	-0.163	-0.205	-0.205
	0.182	0.153	0.121	0.082	0.035	0.035
Au(1)	-0.017	-0.018	-0.018	-0.016	-0.01	-0.01
	0.246	0.245	0.244	0.245	0.253	0.253
H(7)	0.223	0.226	0.229	0.231	0.232	0.234
	0.218	0.219	0.221	0.222	0.224	0.225
H(11)	0.22	0.223	0.225	0.228	0.229	0.231
	0.216	0.217	0.219	0.22	0.222	0.223
H(10)	0.227	0.225	0.223	0.221	0.221	0.22
	0.219	0.218	0.217	0.216	0.216	0.216
H(8)	0.222	0.22	0.218	0.217	0.216	0.215
	0.216	0.215	0.214	0.214	0.213	0.213
H(13)	0.237	0.239	0.24	0.241	0.242	0.243
	0.221	0.222	0.223	0.223	0.224	0.224
H(14)	0.237	0.235	0.234	0.232	0.231	0.231
	0.224	0.223	0.222	0.221	0.22	0.219
H(15)	0.285	0.283	0.281	0.278	0.275	0.272
	0.268	0.266	0.264	0.262	0.261	0.259
H(16)	0.251	0.252	0.252	0.253	0.254	0.253
	0.225	0.226	0.227	0.227	0.228	0.228
H(2)	0.245	0.246	0.246	0.247	0.248	0.25
	0.224	0.224	0.224	0.224	0.224	0.225
H(1)	0.275	0.279	0.284	0.288	0.294	0.301
	0.276	0.279	0.282	0.285	0.288	0.292
H(5)	0.247	0.251	0.254	0.258	0.262	0.267
	0.228	0.23	0.233	0.236	0.239	0.242
H(4)	0.235	0.234	0.233	0.232	0.232	0.232
	0.22	0.219	0.219	0.218	0.218	0.219

*****First row: MPA; Second row: NPA charges

Using these parameters, the I–V characteristics of the DCC molecule has been studied. Figure 10 illustrates the I-V characteristics of DCC molecule for the applied electric fields. It reveals that, as the bias voltage increases, the current increases gradually showing the nonlinear behavior of the molecule. Since DCC is symmetric, the curve is also almost symmetric for both directions of the applied electric field.

Conclusion

This paper describes the effect of external electric field over the electron density, topological and geometrical paarameters and of Au and S substituted DCC based molecular nanowire for various external applied fields (0 - ±0.26 $VÅ^{-1}$) by DFT method using LANL2DZ basis set. For the applied field, the Au−S bond length at the R-end is found slightly longer than the L-end; this difference can be explained in a way that , the Gold atoms at the terminals might get effect strongly due to the applied Electric fields than the same at the R-end. Further, the structural comparison on various Electric fields clearly shows the terminal groups are very sensitive to the EF, whereas the the central DCC is almost insensitive to the EF. The bond topological analysis reveals the variation of electron density $\rho_{bcp}(r)$ and $\nabla^2\rho_{bcp}(r)$ at the bcp of bonds for zero and the different applied fields; although the variations are small, in most cases it is found to be systematic and almost uniform. Further, both HOMO and LUMO levels are approach each other when the field increases from 0.00 to 0.26 $VÅ^{-1}$. When the field increases, it was found that DOS get thicker and HLG decreases from from 2.09 to 0.71 eV which may due to the accumulation of charges or the conduction of electrons from HOMO to LUMO, which reveals the strong conducting nature of the molecule at high applied elecric field. The I-V characteristic curve is found very symmetric and non linear character for the DCC molecule. The effect of electric field over dipole moment indicates that the dipole moment of the molecule increases from 2.50 to 12.45 D. As a conclusion, the Au and Thiol substituted DCC molecule is found to be conducting at higher applied filed.

Acknowledgement

The author ADS is very much grateful to the Department of Science and Technology, SERB for the kind support in doing this research by providing financial assistance under young scientist fast track project scheme.

References

[1] Boon. K. Teoa, Shu-Ping Huang, R..Q. Zhang, Wai-Kee Li, Coordination Chemistry Reviews 253 (2009) 2935.
[2] P. Srinivasan, A. David Stephen, P. Kumaradhas, J. Mol. Struct. (THEOCHEM) 910 (2009) 112.
[3] C. Schubert, J.T. Margraf, T. Clark and D.M. Guldi, Chemical Society Reviews 44 (2015) 988.
[4] P. Tarakeshwar, J.J. Palacios, and Dae M. Kim , IEEE Transactions on Nanotechnology 8 january (2009).
[5] Oxtoby, Gillis, and Campion *Principles of Modern Chemistry*; Sixth Edition. Thomson Brooks/Cole United States (2008) p 224.
[6] Petrucci, Harwood, Herring and Madura *General Chemistry:Principles and Modern Applications*; Ninth edition New jersey (2008)
[7] R.F.W. Bader, *Atoms in molecules - A quantum theory*, Clarendon Press, Oxford (1990).
[8] M.J. Frisch, G.W. Trucks, H.B. Schlegel, G.E. Scuseria, M.A. Robb, J.R. Cheeseman, J.A. Montgomery, Jr. Vreven, K.N. Kudin, J.C. Burant, J.M. Millam, S.S. Iyengar, J. Tomasi, V. Barone, B. Mennucci, M. Cossi, G. Scalmani, N. Rega, G.A. Petersson, H. Nakatsuji, M. Hada, M. Ehara, K. Toyota, R. Fukuda, J. Hasegawa, M. Ishida, T. Nakajima, Y. Honda, O. Kitao, H. Nakai, M. Klene, X. Li, J.E. Knox, H.P. Hratchian, J.B. Cross, C.Adamo, J.Jaramillo, R. Gomperts, R.E. Stratmann, O. Yazyev, A.J. Austin, R. Cammi, C. Pomelli, J.W. Ochterski, P.Y. Ayala, K. Morokuma, G.A. Voth, J. Salvador J. Dannenberg, V.G. Zakrzewski, S. Dapprich, A.D. Daniels, M.C. Strain, O. Farkas, D.K. Malick, A.D. Rabuck, K. Raghavachari, J.B. Foresman, J.V. Ortiz, Q Cui, A G Baboul, S Clifford, J Cioslowski, B Stefanov, G Liu, A Liashenko, P. Piskorz, I. Komaromi, R.L. Martin, D.J Fox, T. Keith, M.A. Al-Laham, C.Y. Peng, A. Nanayakkara, M. Challacombe, P.M.W Gill, B. 47 Johnson, W. Chen, M.W. Wong, C. Gonzalez, J.A. Pople, Gaussian Inc Pittsburgh P A, (2003).
[9] S. Jalili and H. Rafii-Tabar Phys. Rev. B 71 (2005) 165410.
[10] F.W. Biegler-Konig, R.F.W. Bader, T.H. Tang, J. Comput. Chem. 3 (1982) 317
[11] N.O. Boyle, GaussSum, Revision 2.1 (2007).
[12] Y. Zhao, D.G. Truhlar, Accounts of Chemical Research 41 (2008) 157; Y Zhao, D.G. Truhlar, Org. Let.t 9 (2007) 1967.
[13] D. Cremer and E. Kraka, CroatiaChemicaActa 57 (1984) 1259–1281
[14] Karuppanan Selvaraju, Poomani Kumaradhas, Journal of Nanoscience 2015 (2015) 12.
[15] K. Selvaraju, M. Jothi, and P. Kumaradhas, Journal of Computational and Theoretical Nanoscience 11 (2014) 524–532.
[16] A.K . Singh, A. Kumar, P.C. Mishra, Journal of Molecular Structure: THEOCHEM 621 (2003) 261-278
[17] F. Martin and H. Zipse, Journal of Computational Chemistry, 26 (2005) 97–105.
[18] Abraham Nitzan and Mark A. Ratner E Science 300 (2003) 1384.
[19] N. J. Tao, Nature Nanotechnology 1 (2006) 173-181 .
[20] D. Farmanzadeh and Z. Ashtiani, StructuralChemistry 21 (2010) 691–699.
[21] R. K. Pathak and S. R. Gadre, The Journal of ChemicalPhysics 93 (1990) 1770–1773.
[22] P. Politzer and D.G. Thruhlar, *Chemical Applications of Atomic and Molecular ElectrostaticPotential*, PlenumPress, NewYork, NY, USA (1981)
[23] B.Hu, C.Yao and Q.Wang, Journal of Theoretical and ComputationalChemistry, 10 (2011) 829–838.
[24] B. Kirtman, B. Champagne, and D. M. J. Bishop, Journal of the American Chemical Society 122 (2002) 8007–8012.
[25] D. Rai, A.D. Kulkarni, S.P. Gejji, R.K. Pathak, J. Chem. Phys. 128 (2008) 0343101.
[26] L.T. Cai , H. Skulason , J.G. Kushmerick , S.K. Pollack, J.Naciri, R. Shashidhar , D. L. Allara, T. E. Mallouk and T. S. Mayer J. Phys. Chem. B 108 (2004) 2827.
[27] R. Landauer, PhysicsLettersA 85 (1981) 91–93.
[28] M. D. Ganji and A. Mir-Hashemi, Physics Letters, Section A: General, Atomic and Solid State Physics 372 (2008) 3058–3063.
[29] C. Kergueris, J.P. Bourgoin, S. Palacin, D. Esteve, C. Urbina, M. Magoga and C. Joachim, Phys. Rev. B 59 (1999) 12505.